Hindawi
Advances in Civil Engineering
Volume 2023, Article ID 1629681, 10 pages
https://doi.org/10.1155/2023/1629681

Research Article

Numerical Simulation Research and Application of Support Design of Broken Rock Mass in Submarine Gold Mine

Yu-yun Fan[1,2] **Ming-wei Jiang,**[1,2] **Li Cheng**[1,2] **Xi Wang,**[1,2] **Xing-quan Liu,**[1,2] **Chunlong Wang,**[1,2] **and Kexu Chen**[1,2]

[1]*Deep Mining Laboratory of Shandong Gold Group Co., Ltd., Laizhou 261442, China*
[2]*Shandong Key Laboratory of Deep-sea and Deep-earth Metallic Mineral Intelligent Mining, Laizhou 261442, China*

Correspondence should be addressed to Yu-yun Fan; 1066978589@qq.com

Received 26 October 2022; Revised 17 July 2023; Accepted 20 July 2023; Published 10 August 2023

Academic Editor: Dawei Yin

In order to solve the problem that the broken rock mass is easy to collapse and fall during the excavation of a submarine gold mine, two kinds of bolt-mesh-concreting combined support schemes are designed by means of field engineering geological investigation, indoor rock mechanics test, rock mass quality classification, and theoretical analysis. We use the numerical simulation for verification and carry out the field industrial test. The results show that the stability grade of broken surrounding rock is III–IV; both schemes can effectively control the deformation and failure of surrounding rock. Compared with the unsupported scheme, the maximum roof displacement in the scheme using roadway roof and sidewall support is reduced by 26.9%, the maximum thickness of the roof plastic zone is reduced by 58.2%, and the volume of the surrounding rock plastic zone is reduced by 26.32%. The bolt-mesh-shotcrete support has good control effect on the loose deformation of surrounding rock, which can effectively prevent the roof collapse and sidewall spalling of roadway. The field industrial test of support scheme meets the stability control requirements of broken rock mass in mines, and the application effect is obvious. The research results presented in this study provide valuable technical guidance and essential insights for the design of support systems in other similar mining projects, contributing to the effective control and stability of broken rock masses during excavation.

1. Introduction

Rock mass stability is the core issue of underground engineering design. The stability of underground rock after excavation plays an important role in mine safety production, especially roof caving and collapse after excavation, which has always been the most concerning problem in mine safety production. The stability of rock mass after excavation is a difficult problem in the study of mine ground pressure management. Roof caving and collapse accidents are closely related to mining environment, geological factors, mining methods, and roof support control methods [1–3]. Aiming at the stability control problem of broken rock mass, scholars at home and abroad have done much research and exploration. Sheng et al. [4] analyzed and studied the roadway with strong plastic broken rock mass and formed a coupling support method combining prestressed anchor, steel wire mesh, shotcrete, grouting, and pressure relief groove. Zhang et al. [5] analyzed the roadway support under the condition of an empty area around the seabed roadway and proposed the integrated support technology of shotcrete-bolting and piercing. Tian [6] proposed the deep-shallow rigid-flexible coupling bolt-grouting support technology for high-stress roadways in view of the large deformation of surrounding rock and the serious failure of support structure in deep high-stress roadway; Zuo et al. [7] proposed the graded control principle and yield failure criterion of surrounding rock gradient support and realized the graded three-dimensional pressure shell control of surrounding rock based on gradient failure mechanism. Meng et al. [8] revealed the deformation and failure characteristics of deep high-stress broken soft rock roadway and put forward the step-by-step combined support technology scheme of "anchor net cable shotcrete + U steel support + grouting + floor anchor grouting." Zhang et al. [9] used the numerical simulation to study the stress and displacement variation law of roadway under different surrounding rocks, aiming to determine the

Figure 1: Existing supporting methods of broken rock mass.

reasonable roadway support method. Hui and Li [10] provided the calculation formula of the permanent support scope when the mine roadway passed through the loose and broken zone. At present, the research on the stability control technology of fractured rock mass in submarine gold mines is still insufficient [11–16]. However, there have been many important advances in rock mechanics and support engineering in the past 5 years, such as the techniques and strategies proposed in the study of rock stability [17–21]. In addition to static loads, dynamic factors are also important factors affecting rock stability, such as microseisms caused by fault slippage or ground vibrations caused by blasting [22–25].

This paper uses a broken rock mass in the southwest wing of a seabed metal mine as the research background. Through field engineering geological survey, laboratory rock mechanics test, rock mass quality classification, theoretical analysis, and other means and methods, the corresponding high-stress coupling support scheme is designed, the numerical simulation is used to verify, and the field industrial test is carried out. The aim is to ensure the stability of the roadway surrounding rock support and enhance the efficiency of roadway excavation. This research provides valuable technical support for the excavation and stability control of roadways in broken-rock conditions. Additionally, it aims to reduce support costs and improve the safety of mining operations.

2. Engineering Background

The structure controls the ore body of a submarine gold deposit before and during mineralization. The mineralization intensity is closely related to the fragmentation degree of altered rock and the development degree of metallogenic fracture. The high-grade part and the thickness of the ore body are mostly the areas with developed metallogenic fracture and strong rock fragmentation. The ore body is distributed in the pyrite sericitization catacaustic rock belt with strongly altered rock fragmentation and developed metallogenic fracture under the main fracture surface. Some areas are affected by seawater pressure and internal seepage of rock mass, and the rock strata movement law is complex [5], which is more likely to cause the caving and collapse of the roof fracture area. The transportation roadway outside the southwest wing vein is located in the area of the broken rock mass. The joint fissure is developed, the rock mass strength is low, and the joint is filled with alteration. The alteration is affected by water (after water, it expands and produces slippery). The fracture expansion is low and easy to collapse. If the support is not timely or the support scheme is unreasonable, it may cause the collapse to further extend upward and gradually approach or even lead to the seabed strata, resulting in large area of seawater recharge [10]. Therefore, timely and effective support measures to control roadway surrounding rock and maintain long-term stability are the key problems to be solved urgently.

At present, in view of the broken ore body, the excavation method of the mine mainly adopts the collision wedge method and the pipe shed method. The steel arch, shotcrete, metal mesh, and other combined support methods are used (Figure 1). The support cost is relatively high, the excavation speed is slow, and the excavation speed of the mine is seriously restricted.

3. Rock Mass Quality Evaluation and Rock Mechanics Parameter Estimation of the Surrounding Rock

3.1. Indoor Rock Mechanic Test. In order to accurately obtain the basic rock mechanical parameters of the rock mass in the transportation roadway area of the southwest wing, typical rock samples were collected from the transportation roadway and the heading face of the mining connection. The roof positions of the working face of the transportation roadway in the southwest wing of −212, −307, and −373 m sections were sampled, respectively. We mainly selected intact rocks with fewer original joints and fissures. Three rock samples were taken at each level, and a total of nine rock samples were obtained.

The rock samples are processed into standard rock specimens. We carried out the uniaxial compression, Brazilian splitting, and triaxial compression tests by using ZTR-276 rock triaxial testing machine and rock mechanics universal testing machine (Figure 2). The basic rock mechanics parameters are obtained, as shown in Table 1.

3.2. Quality Evaluation of Surrounding Rock Mass. Through the field engineering geological survey, the structural plane information of roadway surrounding rock is measured, counted, and

(a) (b)

Figure 2: Laboratory rock mechanics test instrument: (a) ZTR-276 rock triaxial testing machine and (b) rock mechanics universal testing machine.

Table 1: Rock physical and mechanical parameters of indoor rock mechanic test.

Specimen position	Density (kg/m^3)	Uniaxial compressive strength (MPa)	Tensile strength (MPa)	Elastic modulus (GPa)	Poisson's ratio	Intensive parameter	
						c/MPa	φ
−212 m level	2,718	39.18	5.3	33.85	0.235	8.48	40.4
−307 m level	2,722	45.52	4.9	38.75	0.23	15.63	41.4
−373 m level	2,748	78.15	5.9	44.90	0.22	10.62	50.8

Table 2: Comparison of classification results of three rock mass evaluation methods.

Position	RMR			Q		GSI
	Grade	Description	Stability	Grade	Description	GSI value
−200 m	IV	Bad	(2.5 m span) 10 hr	IV	Very bad	39 (36–42)
−240 m	IV	Bad	(2.5 m span) 10 hr	IV	Very bad	39 (36–42)
−280 m	IV	Bad	(2.5 m span) 10 hr	IV	Very bad	44 (45–53)
−320 m	IV	Bad	(2.5 m span) 10 hr	IV	Very bad	47 (45–53)
−360 m	III	Not very bad	(5 m span) 7 days	III	Bad	56 (50–70)
−400 m	III	Not very bad	(5 m span) 7 days	III	Bad	56 (50–70)
−440 m	III	Not very bad	(5 m span) 7 days	III	Bad	63 (50–70)

analyzed by using the line measurement method and statistical window method, and the distribution characteristics of joints and fissures in different levels of the surrounding rock are mastered. According to the survey results, we use the Rock Mass Rating (RMR), Q-system (Q), and Geological Strength Index (GSI) classification methods to classify the stability of the roadway broken surrounding rock at −200 to −440 m in the southwest wing. The results are shown in Table 2. At southwest wing roadway surrounding rock quality grade III–IV, rock stability is very poor; the joint fissures of surrounding rock are very developed, and its stability is mainly controlled by joint fissures.

3.3. Estimation of Mechanical Parameters of Rock Mass. According to the indoor rock mechanics test and rock mass quality evaluation results, the reduction method based on rock mass quality evaluation and the systematic Hoek–Brown criterion estimation method are used to estimate the rock mass mechanical parameters. The average value of the calculated values of the two methods is taken as the final rock mass parameters.

When using the reduction method based on rock mass quality evaluation to estimate rock mass mechanical parameters, it is necessary to first collect mechanical test data related to rock mass samples, reduce the data, calculate the minimum principal stress, use a rock classification system to estimate rock mass strength parameters, and finally conduct sensitivity analysis to understand the reliability of the estimation results. The Hoek–Brown criterion estimation method requires first determining the rock mass properties and then using the empirical formula of the Hoek–Brown criterion to calculate the rock mass parameters based on the characteristics of the rock sample.

Due to the limited field sampling, the rock sample parameters are used to represent the rock parameters of the nearby level: the rock samples of −212 m level represent the rock properties of −200 and −240 m middle sections;

Table 3: Estimation results of physical and mechanical parameters of fractured rock mass in the southwest wing.

Position	Density (t/m^3)	Uniaxial compressive strength (MPa)	Tensile stress (MPa)	Elastic modulus (GPa)	Poisson's ratio	Intensive parameter	
						c/MPa	φ/(°)
−200 m	2.718	9.58	0.08	5.5	0.235	2.90	35.7
−240 m		8.87	0.07	5.3		2.83	35.1
−280 m	2.722	8.68	0.18	4.4	0.230	3.45	36.3
−320 m		8.55	0.27	4.5		3.49	36.6
−360 m	2.748	16.24	1.99	10.4	0.220	6.95	39.3
−400 m		17.74	2.11	11.8		7.06	39.8
−440 m		18.86	5.54	13.4		7.40	40.6

rock samples at the −307 m level represent rock properties at −280 and −320 m intervals; and rock samples of −373 m level represent rock properties of −360, −400, and −440 m middle sections. The estimation results of rock mechanics parameters are shown in Table 3.

4. Support Scheme Design and Numerical Simulation Analysis

4.1. Support Scheme Design. Based on the field engineering geological investigation, support method investigation, and rock mass quality evaluation results and according to the relevant theoretical calculation, design specification, and engineering analogy method, the bolt-mesh-shotcrete combined support is selected, and two support schemes are designed to ensure the stability and safety of the roadway.

Scheme A: Bolt-mesh-shotcrete combined support, roadway roof and sidewall are using Φ 20 × 2,200 mm resin bolt support, the row spacing is 1,000 × 1,000 mm, metal mesh specification is Φ 4 @ 50 × 50 mm, concrete spray layer thickness is 50 mm, and a total of nine bolts per row.

Scheme B: Bolting and shotcrete support, only supporting roadway roof, roadway two sides do not support; the parameters of bolt, double ribs, and shotcrete are the same as that of support scheme A, with five bolts per row.

4.2. Numerical Model and Boundary Conditions. We use FLAC3D to simulate the support scheme. FLAC3D is a numerical simulation method based on the finite difference method used to solve mechanical problems in geotechnical and geological engineering. Based on the principle of combining particle fluid mechanics with the finite element method, the problem area is discretized and meshed. FLAC3D can simulate the deformation and fracture behavior of rock and soil, and obtain relevant parameters such as stress and strain at each node for analyzing the stability of the structure.

Because two adjacent roadways are close to each other in the buried depth (the thickness of isolated rock mass is about 10 m), considering the influence of adjacent roadway excavation on the stability of surrounding rock, two segment transport roadways in the middle (40 m) are selected as the simulation objects. The calculation area of the model is 30 × 10 × 40 m (length × width × height), and the excavation section of the roadway is 3.6 × 3.3 m. There are 106,785 nodes and 100,320 units. The model adopts the ideal elastic–plastic rock mass, and the plain concrete support with an appropriate increase in mechanical parameters represents the metal mesh shotcrete support. In the numerical calculation, shell element is used to simulate shotcrete and pile element is used to simulate bolt support. The vertical displacement constraint is applied at the bottom of the model, and the horizontal displacement constraint is applied at the vertical boundary before and after the model. Figure 3 shows the overall and support model for numerical calculations.

We select the −360 m level with the worst surrounding rock condition in the southwest wing of the mine for the support scheme simulation. The simulation schemes are no support, scheme A and scheme B, respectively. The value of ground stress is referred to the measured ground stress value of the mine, as shown in Table 4. The numerical simulation parameters refer to the estimated values of rock mechanics parameters in Table 3, as shown in Table 5.

4.3. Numerical Simulation Results and Analysis. Figures 4 and 5 show that the surrounding rock of the roadway is mainly in compressive stress state, and there is a small tensile stress in some rock walls. The stress concentration of surrounding rock is mainly at the two corners of arch shoulder and floor, and the stress concentration in the vertical direction is much more obvious than that in the horizontal order. Compared with before support, the maximum value of surrounding rock compressive stress changes little after support, but the stress concentration position moves to the free face of roadway, and the stress value at the roof increases, indicating that bolt-mesh-shotcrete support effectively prevents the deformation and loosening of surrounding rock, resulting in the increase of shallow compressive stress of surrounding rock.

We can see from Figures 6–8 that the convergence deformation of surrounding rock after support is also reduced compared with that without support, and the range of the plastic zone is also degenerated, especially the thickness of the roadway roof plastic zone is significantly reduced. The deformation displacement of the roof is reduced from 12.73 to 9.31 mm, and the convergence of the sidewall is reduced from 13.13 to 11.28 mm (see Table 6). It shows that the bolt-mesh-shotcrete support has a good control effect on the loose deformation of the surrounding rock, which can effectively

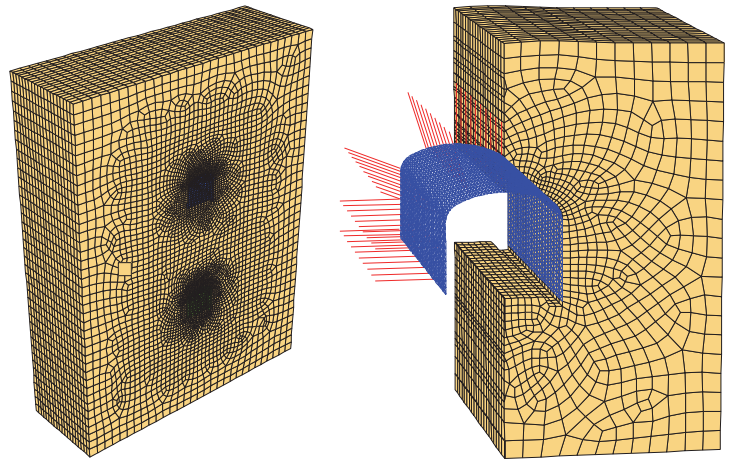

(a) (b)

Figure 3: Numerical models: (a) overall model and (b) support model.

Table 4: The value of −360 m level ground stress.

Position	Maximum horizontal principal stress σ hmax (MPa)	Vertical stresses σ z (MPa)	Minimum horizontal principal stress σ hmin (MPa)
−360 m level	19.514	11.42	6.646

Table 5: Value of main parameters in numerical simulation.

Material categories	Density (t/m^3)	Elastic modulus (GPa)	Poisson's ratio	Tensile stress (MPa)	Cohesion (MPa)	Internal friction angle (°)
−360 m rock	2.748	10.4	0.220	1.99	6.95	39.3
Bolt	7.85	200	0.28	390		
Metal mesh-sprayed concrete	2.50	40	0.25	2.70		

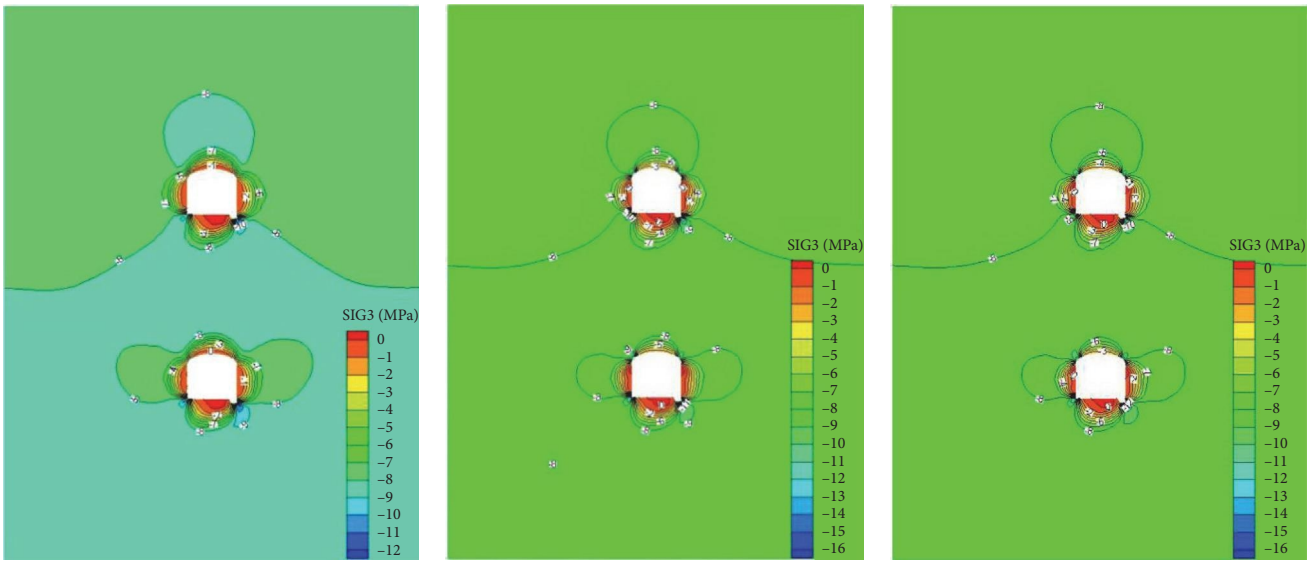

(a) (b) (c)

Figure 4: The maximum principal stress nephogram of surrounding rock under different support conditions at −360 m level: (a) unsupported, (b) scheme A (nine bolts per row), and (c) scheme B (five bolts per row).

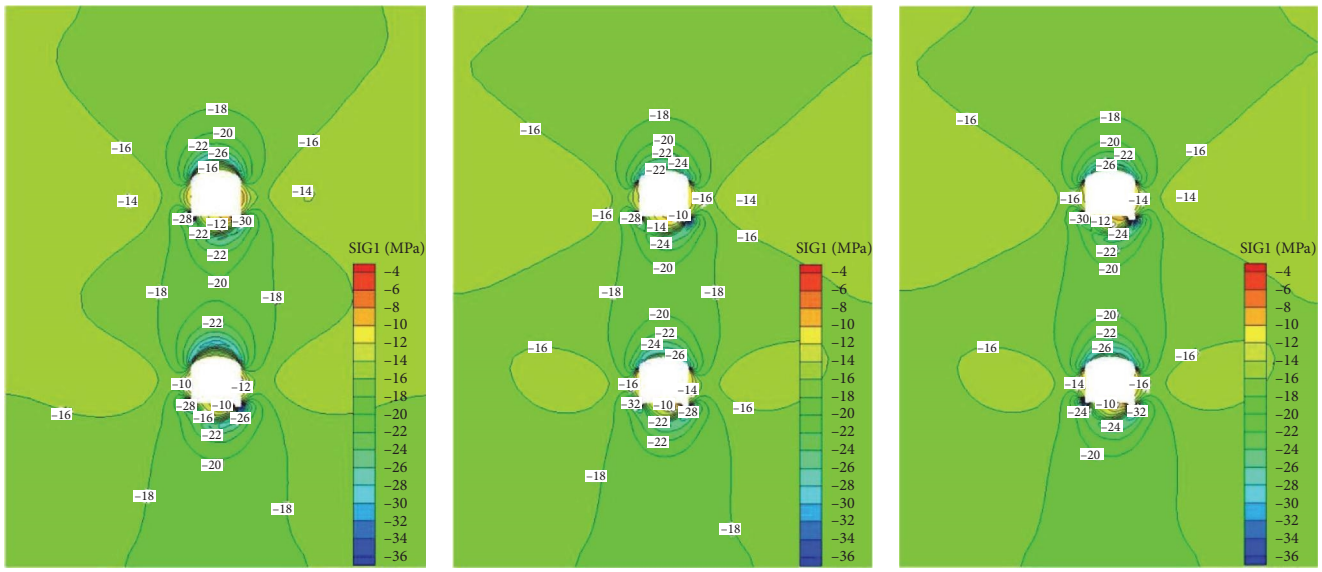

(a) (b) (c)

Figure 5: The minimum principal stress nephogram of surrounding rock under different support conditions at −360 m level: (a) unsupported, (b) scheme A (nine bolts per row), and (c) scheme B (five bolts per row).

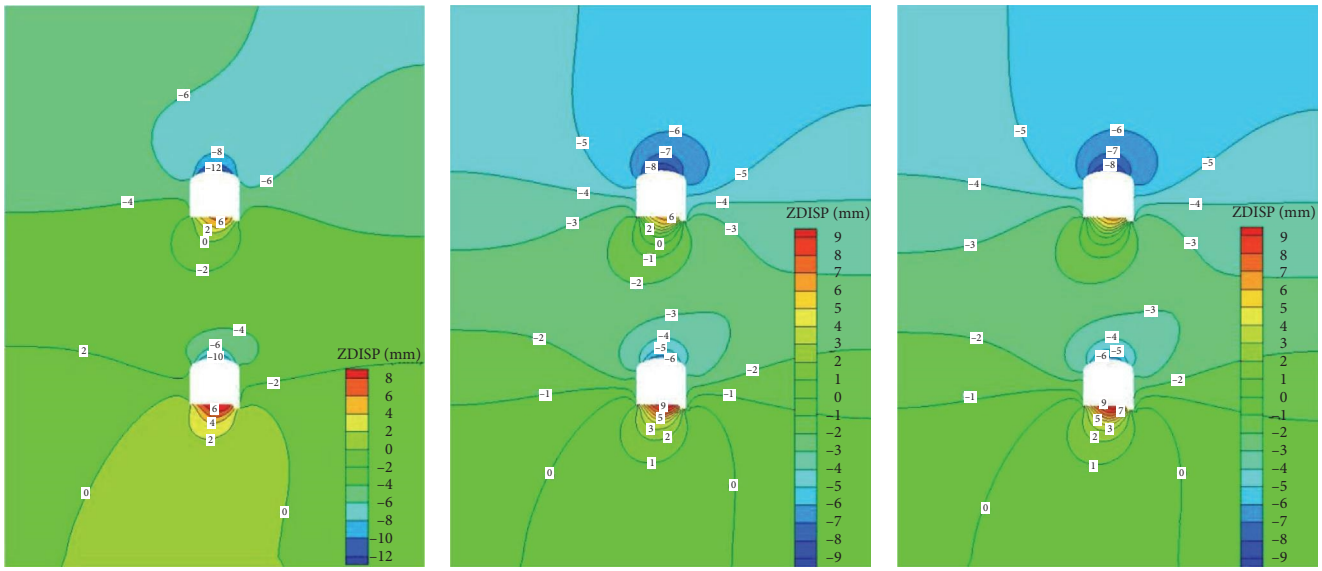

(a) (b) (c)

Figure 6: Vertical displacement of surrounding rock under different support conditions at −360 m level: (a) unsupported, (b) scheme A (nine bolts per row), and (c) scheme B (five bolts per row).

prevent the roof collapse and sidewall spalling of the roadway. Scheme B only supports the roof of the roadway, and the deformation control of the two sides of the roadway is not as obvious as scheme A. The convergence of the sidewall is reduced from 13.13 to 11.34 mm. The maximum lateral displacement of the two support schemes decreases by 14.1% (scheme A) and 13.6% (scheme B), respectively. There is no significant difference between the two schemes, and the support cost of scheme B is lower than that of scheme A. Therefore, when the surrounding rock of roadway only needs roof support or two sides of rock mass conditions are good, support scheme B should be preferred.

We can see from the above table that bolt-mesh-shotcrete support effectively controls the loose deformation of roadway surrounding rock and strengthens the overall strength of rock mass. With the increase of support strength, the principal stress of rock mass increases gradually, and the convergence displacement of surrounding rock decreases gradually, especially the maximum displacement of roof decreases by 26.9% (scheme A). When the roadway is not

(a) (b) (c)

Figure 7: Horizontal displacement of surrounding rock under different support conditions of −360 m level: (a) unsupported, (b) scheme A (nine bolts per row), and (c) scheme B (five bolts per row).

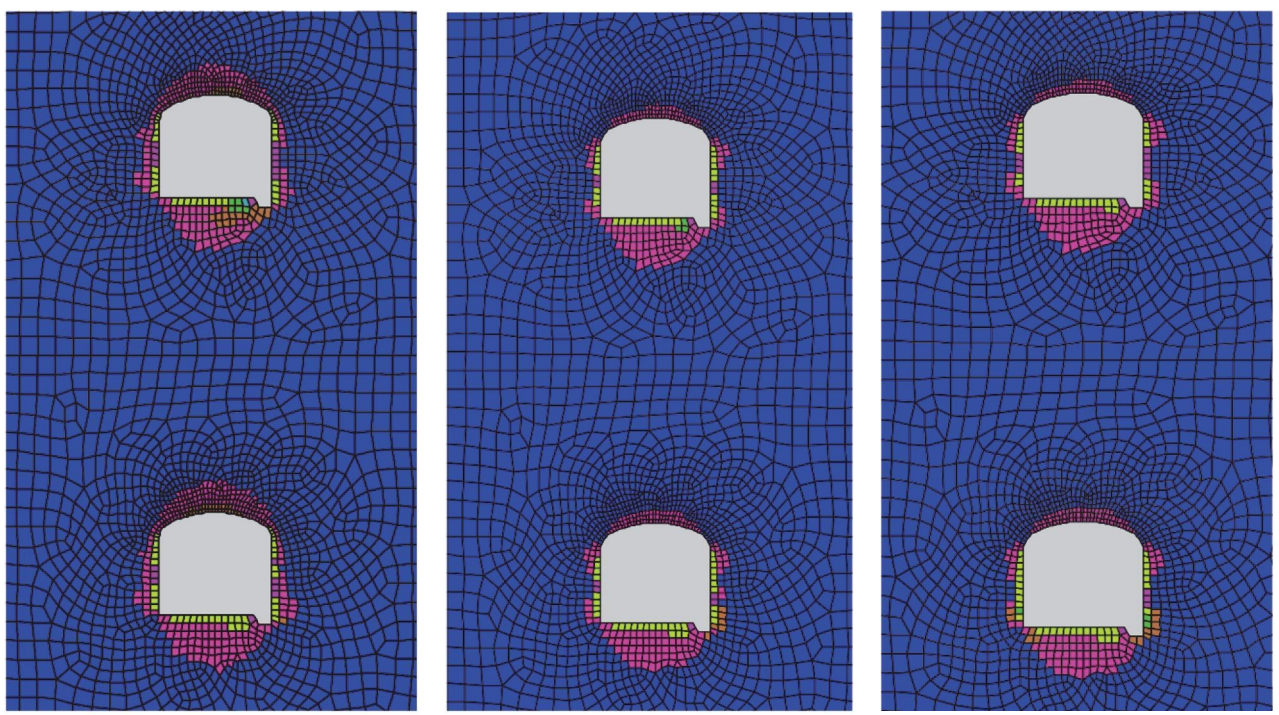

(a) (b) (c)

Figure 8: Cloud image of the plastic zone of surrounding rock under different supporting conditions at −360 m level: (a) unsupported, (b) scheme A (nine bolts per row), and (c) scheme B (five bolts per row).

Table 6: Comparison table of simulation results of surrounding rock under different supporting conditions.

Position	Support scheme	Minimum principal stress (MPa)	Maximum principal stress (MPa)	Maximum roof displacement (mm)	Maximum lateral wall displacement (mm)	Maximum thickness of roof plastic zone (m)	Plastic zone volume of the surrounding rock (m^3)
	Unsupported	−33.89	0.48	12.73	13.13	1.03	253.30
−360 m	Scheme A	−33.50	0.89	9.31	11.28	0.43	186.63
	Scheme B	−33.48	0.94	9.37	11.34	0.50	191.81

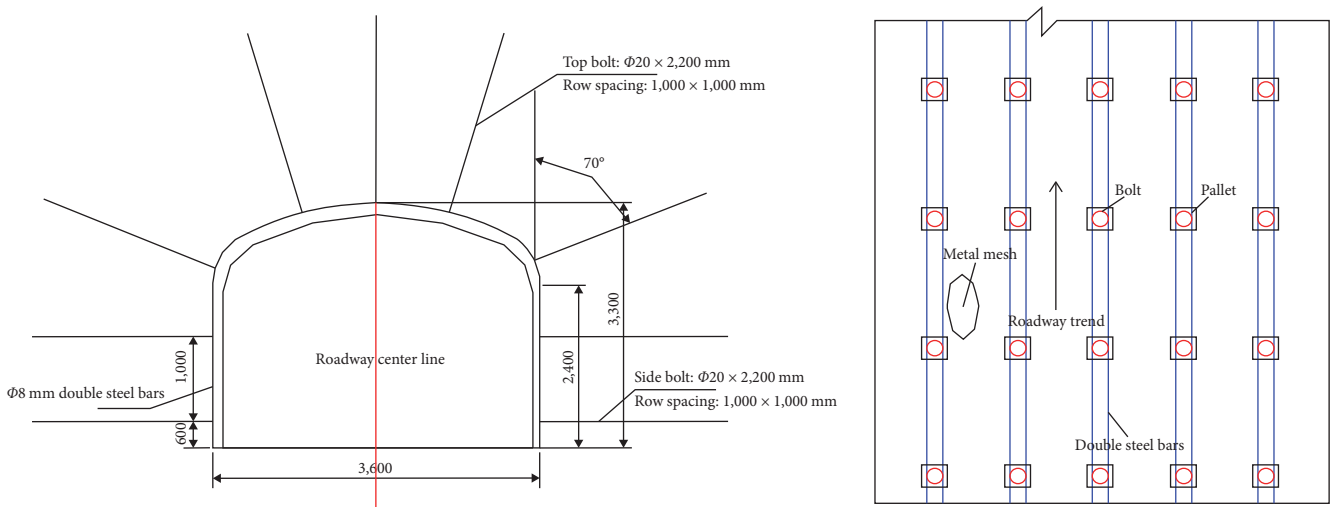

Figure 9: −212 m horizontal test roadway anchor net spray support design.

supported, the maximum thickness of the roof plastic zone is 1.03 <2.20 m and the bolt length meets the safety standard. After support, the maximum thickness of plastic zone of roof is reduced by 58.2%, and the volume of plastic zone of surrounding rock is reduced by 26.32% (scheme A), and the reinforcement effect is remarkable.

5. Site Industrial Test

5.1. Design of Test Area and Support Parameters. According to the field engineering geological investigation and statistical analysis of the broken area, combined with the rock mass quality evaluation at the test site and its nearby area, the combined support method of bolt + metal mesh + shotcrete was determined to strengthen the surrounding rock of roadway at the test site at the level of −212 m. Parameters of bolt-mesh-shotcrete combined support: Φ 20 × 2,200 mm resin bolt is selected for roadway roof and sidewall, and the distance between them is 1,000 × 1,000 mm. After installing the bolt, the metal mesh is mounted along the arch ring, and the double bars are installed along the direction of the roadway. Finally, the 50 mm thick concrete closed support structure and surrounding rock are sprayed (as shown in Figure 9).

5.2. Test Result Analysis. In order to highlight the effectiveness and economy of bolt-mesh-shotcrete combined support, the field test effect at −212 m level was compared with that of U-shaped steel arch support at −228 m level.

As shown in Figures 10 and 11, it can be seen that compared with U-shaped steel arch support, bolt-mesh-shotcrete combined support can not only ensure the lasting stability of broken surrounding rock of roadway, but also has better support effect and can better meet the special requirements of roadway excavation and maintenance in broken rock mass.

Compared with the construction cost (Table 7) of the two supporting methods, anchor mesh shotcrete support also shows great economic advantages.

6. Conclusions

(1) The rock mass stability grade of the broken surrounding rock in the southwest wing has been determined as III–IV using various rock mass quality classification methods (RMR, Q, and GSI). The evaluation of rock mass mechanical parameters using the reduction method of rock mass quality evaluation and the systematic Hoek–Brown criterion estimation method provides essential data for subsequent numerical simulation analysis of support schemes.

(2) Two bolt-mesh-shotcrete combined support schemes, A and B, were designed based on support methods investigation and rock mass quality evaluation. Numerical simulations indicate that this support system effectively controls deformation and enhances overall rock mass strength. As support strength increases, principal stress

Figure 10: −212 m horizontal test roadway anchor net spray support effect.

Figure 11: −228 m horizontal U-shaped steel arch support effect.

Table 7: Comparison table under different supporting conditions.

Supporting position	Support way	U-shaped steel (bolt) row number	Support length (m)	Total support costs (yuan) (including labor costs)	Support unit price (yuan/m) (including labor costs)	Construction personnel
−212 m level	Bolt-mesh-spurting supporting	9	7	5,640.5	805.79	Drilling and bolt installation 2; net 3
−228 m level	U-shaped steel support	8	8.6	15,338.2	1,783.5	10

gradually rises, and convergence displacement decreases. Scheme B is recommended for grade III rock mass when roof support is necessary, while scheme A is favored for grade IV rock mass if the sidewall condition is better but the roof is unstable. The numerical simulations demonstrate the reliability and effectiveness of the anchor mesh shotcrete support scheme.

(3) Field industrial tests confirm that the designed bolting-mesh-spraying support scheme effectively stabilizes fractured rock mass, give full play to self-stability of surrounding rock, and exhibits remarkable support performance. Compared to adjacent horizontal roadway support methods, anchor net shotcrete support demonstrates advantages such as lower cost, simplicity, rapid construction, and improved economics. This scheme can serve as technical guidance for similar mining areas.

Data Availability

Data supporting this research article are available from the corresponding author on reasonable request.

Conflicts of Interest

The authors declare that they have no conflicts of interest.

Acknowledgments

National Key Research and Development Plan: Key technologies for well construction and lifting in deep metal mines (No. 2016YFC 0600800). Major Scientific and Technological Innovation Project of Shandong Province' s key technology and equipment integration research and engineering application of intelligent mining of deep metal mines (No. 2019SDZY05).

References

[1] X. X. Chen and J. P. Wu, "Study on the mechanism and control technology of large deformation of roadway surounding rock in the fault fracture zone," *Journal of Mining & Safety Engineering*, vol. 35, no. 5, pp. 885–892, 2018.

[2] Z. Jin-feng and Z. Peng-hao, "Analytical model of fully grouted bolts in pull-out tests and in situ rock masses," *International Journal of Rock Mechanics and Mining Sciences*, vol. 113, pp. 278–294, 2019.

[3] Q. Wang, B. Jiang, R. Pan et al., "Failure mechanism of surrounding rock with high stress and confined concrete support system," *International Journal of Rock Mechanics and Mining Sciences*, vol. 102, pp. 89–100, 2018.

[4] J. Sheng, Q. Li, H. Zhang, D. Liu, and G. Zhao, "Study and application of coupling support technology for the roadway with broken and strong-plasticity rock mass," *Mining Research and Development*, vol. 40, no. 8, pp. 91–96, 2020.

[5] C. Zhang, W. Song, J. Fu, Y. Li, and K. Zhang, "Technology for roadway management of fractured rock masses in a submarine gold mine," *Journal of Mining and Strata Control Engineering*, vol. 2, no. 3, Article ID 033039, 2020.

[6] W. Tian, "Research on deep - shallow rigid - flexible coupling anchor - grouting support technology for deep high stress roadway," *Coal Technology*, vol. 41, no. 3, pp. 18–21, 2022.

[7] J. Zuo, Z. Hong, M. Yu, H. Liu, and Z. Wang, "Gradient support model and classification control of broken surrounding rock," *Journal of China University of Mining and Technology*, vol. 51, no. 2, pp. 221–231, 2022.

[8] Q. Meng, L. Han, J. Zhang, S. Wen, F. Zhang, and H. Li, "Research and application of supporting technology in deep hing stress fractured soft-rock roadway," *Joumal of Central South University (Nature Science Edition)*, vol. 47, no. 11, pp. 3861–3872, 2016.

[9] F. Zhang, H. Zhang, Z. Xia, and S. Wang, "Research on surrounding rock support and control technology for submarine deep well tunnel," *Modern Mining*, vol. 39, no. 4, pp. 171–174, 2023.

[10] A. Hui and M. Li, "Engineering geological environment reconstruction and tunnel construction technology in caving rock mass," *Well Construction Technology*, vol. 42, no. 1, pp. 20–24, 2021.

[11] H. Tian, W. Chen, X. Tan, H. Wang, and T. Tian, "Study on reasonable supporting scheme of high ground stress soft rock tunnel," *Rock Mechanics and Engineering*, vol. 30, no. 11, pp. 2285–2292, 2011.

[12] W. Qi, Q. Zhu, X. Zhao, and W. Li, "Numerical simulation study on stability control of fractured rock mass in southwest wing of Xinli mining area of Sanshandao Gold Mine," *Nonferrous Metals (mining part)*, vol. 71, no. 4, pp. 88–94, 2019.

[13] J. Dong, X. Feng, X. Zhang, and Z. Zhang, "Stability evaluation and parameter optimization of fractured rock mass in underground stope," *Journal of Northeastern University (Natural Science Edition)*, vol. 34, no. 9, pp. 1322–1326, 2013.

[14] R. Pan, "Research on bolting and grouting mechanism and control technology of broken surrounding rock in deep roadway," *Journal of Rock Mechanics and Engineering*, vol. 40, no. 4, Article ID 864, 2021.

[15] H. Luo, R. Wu, Q. Wang, and P. Zhang, "Numerical simulation of stress evolution and surrounding rock control technology in deep broken roadway," *Mining Research and Development*, vol. 41, no. 2, pp. 39–44, 2021.

[16] D. Wu, Y. Li, Y. Qian, C. Fan, and E. Dong, "Study on surrounding rock control technology of deep broken rock roadway," *Metal Mine*, vol. 08, pp. 1–7, 2020.

[17] S. Liu, X. Li, D. Wang, and D. Zhang, "Investigations on the mechanism of the microstructural evolution of different coal ranks under liquid nitrogen cold soaking," *Energy Sources, Part A: Recovery, Utilization, and Environmental Effects*, pp. 1–17, 2020.

[18] X. Zhou, S. Wang, X. Li et al., "Research on theory and technology of floor heave control in semicoal rock roadway: taking Longhu coal mine in Qitaihe mining area as an example," *Lithosphere*, vol. 2022, no. Special 11, Article ID 3810988, 2022.

[19] S. Wang, X. Li, and Q. Qin, "Study on surrounding rock control and support stability of ultra-large height mining face," *Energies*, vol. 15, no. 18, Article ID 6811, 2022.

[20] X. Li, S. Chen, S. Wang, M. Zhao, and H. Liu, "Study on in situ stress distribution law of the deep mine: taking Linyi mining area as an example," *Advances in Materials Science and Engineering*, vol. 2021, p. 11, Article ID 5594181, 2021.

[21] H. Liu, B. Zhang, X. Li et al., "Research on roof damage mechanism and control technology of gob-side entry retaining under close distance gob," *Engineering Failure Analysis*, vol. 138, Article ID 106331, 2022.

[22] J. Ma, L. Dong, G. Zhao, and X. Li, "Discrimination of seismic sources in an underground mine using full waveform inversion," *International Journal of Rock Mechanics and Mining Sciences*, vol. 106, pp. 213–222, 2018.

[23] J. Ma, L. Dong, G. Zhao, and X. Li, "Ground motions induced by mining seismic events with different focal mechanisms," *International Journal of Rock Mechanics and Mining Sciences*, vol. 116, pp. 99–110, 2019.

[24] J. Ma, L. Dong, G. Zhao, and X. Li, "Qualitative method and case study for ground vibration of tunnels induced by fault-slip in underground mine," *Rock Mechanics and Rock Engineering*, vol. 52, pp. 1887–1901, 2019.

[25] J. Ma, L. Dong, G. Zhao, and X. Li, "Focal mechanism of mining-induced seismicity in fault zones: a case study of Yongshaba mine in China," *Rock Mechanics and Rock Engineering*, vol. 52, pp. 3341–3352, 2019.